Tribology International 101 (2016) 204–217

Contents lists available at ScienceDirect

Tribology International

journal homepage: www.elsevier.com/locate/triboint

Coefficient of friction equation for gears based on a modified Hersey parameter

Carlos M.C.G. Fernandes [a,*], Ramiro C. Martins [a], Jorge H.O. Seabra [b]

[a] INEGI, Universidade do Porto, Campus FEUP, Rua Dr. Roberto Frias 400, 4200-465 Porto, Portugal
[b] FEUP, Universidade do Porto, Rua Dr. Roberto Frias s/n, 4200-465 Porto, Portugal

ARTICLE INFO

Article history:
Received 22 December 2015
Received in revised form
29 February 2016
Accepted 25 March 2016
Available online 9 April 2016

Keywords:
Coefficient of friction
Gears
Hersey parameter
Power loss

ABSTRACT

The present work is first of all a bibliographic revision about the coefficient of friction equations for gears. The available expressions were compared and used to predict experimental results trying to draw an overview about the main advantages and disadvantages of each method.

A load sharing function to predict the coefficient of friction was developed based on a modified Hersey parameter. A coefficient of friction equation is then proposed trying to improve the existing methods, including the influence of the oil pressure–viscosity parameter, on the coefficient of friction.

The new equation correlates very well with the experimental results.

1. Introduction

The fuel economy is becoming of great importance for modern civilisations. The actual consumption of fuels is destroying the atmosphere due to the amount of CO_2 emitted. In order to consume less fuel it is necessary to put some effort on the machine's efficiency. From the daily car up to a modern wind turbine, a gearbox or other kind of mechanical device is usually used to achieve a desired operating condition. In order to reduce the economic and environmental impact of fuel consumption, more efficient gears are needed since they are the most relevant source of power loss inside a gearbox, both due to load and no-load losses [1].

The first studies of efficiency in gear transmissions were performed by Weisbach and Gordon [2] and Reuleaux [3] in the 19th century. Around 1950, Earl Buckingham [4] measured the power loss in gears and developed formulas to evaluate the friction losses.

Several authors [1,5,6] presented experimental results concerning power loss of gears. Petry-Johnson et al. [5] presented an experimental investigation of spur gear efficiency with different geometries and different surface finishing and showed that lower modules promoted a reduction in the meshing gear power loss and that a chemically finished gear had better efficiency than a grounded surface gear.

An analytical and experimental investigation on the effects of geometry on sliding losses of spur gears was presented by Yenti et al. [6] showing that decreasing the module can increase the efficiency of a spur gear pair. Additionally, they showed that the pressure angle increase also reduces the meshing gears power loss. Yenti et al. used the Palmgren model to estimate the rolling bearing losses and concluded that the DIN 3990 [7] coefficient of friction is reliable to predict the actual gear meshing power loss.

From the published works it is possible to analyse the influence of the operating conditions on the coefficient of friction. Martins et al. [8] showed that the coefficient of friction decreases with increasing rotational speed and increases with increasing load. Naruse [9] showed that the coefficient of friction is insensitive to changes in the surface roughness (R_a) between 0.5 and 3 μm, while Xiao et al. [10] suggested that the coefficient of friction is lower for lower surface roughness. However, the Naruse and Xiao works were not totally conclusive since they performed only few experimental tests.

In the present work a new equation for the coefficient of friction of meshing gear is developed. Different expressions are presented and compared with experimental results aiming to support the new equation proposed.

2. Meshing gears power loss

A gearbox transmits a given input power (P_{in}) from the input shaft of the driving gear. The mechanism dissipates energy and the driven gear only transmits an output power (P_{out}) lower than the input power. The efficiency of such gear pair is then given by the

* Corresponding author.
E-mail address: cfernandes@inegi.up.pt (C.M.C.G. Fernandes).

http://dx.doi.org/10.1016/j.triboint.2016.03.028
0301-679X/

Notation and units

a	centre distance (mm)
b	gear face width (mm)
h_0	central film thickness (m)
h_{0C}	corrected central film thickness (m)
h_m	minimum film thickness (m)
F_N	gear normal force in each meshing position along the path of contact (N)
f_N	gear normal force per unit contact length in each meshing position along the path of contact (N/mm)
F_{bt}	gear tangential force on the base plane (N)
H_{VL}	local gear loss factor (–)
H_p	hydraulic parameter (mm^{-1})
i	gear ratio (–)
m	gear module (mm)
n	rotational speed (rpm)
p_h	maximum Hertz pressure (GPa)
P_{in}	input power (W)
p_{max}	maximum Hertz pressure (kg/cm^2)
P_{out}	output power (W)
P_V	total power loss (W)
P_{VX}	auxiliary losses (W)
P_{VZ0}	no-load gears power loss (W)
P_{VZP}	meshing gears power loss (W)
P_{VL}	rolling bearings power loss (W)
P_{VD}	seals power loss (W)
p_b	gear base pitch (mm)
p_{bt}	gear transverse base pitch (mm)
R_a	average surface roughness (μm)
R_q	root mean square roughness (μm)
R_z	roughness based on the five highest peaks and lowest valleys over the entire sampling length (μm)
S_p	modified Hersey parameter (–)
S_g	gear geometric parameter (–)
s	pressure–viscosity parameter (–)
t	pressure–viscosity parameter (–)
v_g	gear sliding velocity in each meshing position along the path of contact (m/s)
v_r	gear rolling velocity in each meshing position along the path of contact (m/s)
v_{tb}	gear tangential velocity on the base plane (m/s)
$v_{\Sigma C}$	sum of the gear surface velocities on the pitch point (m/s)
X_L	lubricant factor (/)
x	meshing contact position along the path of contact (mm)
x_Z	gear profile shift (/)
Z	gear number of teeth (/)
α	pressure–viscosity coefficient (Pa^{-1})
α_t	thermal expansion coefficient (/)
α_Z	gear pressure angle (°)
β_b	base helix angle (°)
β_Z	gear helix angle (°)
η	dynamic viscosity (Pa s)
η_Z	efficiency of a gear pair (/)
Λ	specific film thickness (/)
μ_{bl}	coefficient of friction in boundary film lubrication (/)
μ_{EHD}	coefficient of friction in full film lubrication (/)
μ_{mZ}	average meshing gear coefficient of friction (/)
μ_Z	meshing gear coefficient of friction along the path of contact (/)
ν	kinematic viscosity (cSt)
ρ	density (g/cm^3)
ρ_{redC}	equivalent curvature radius on the pitch point (mm)

Subscripts

1, 2	pinion, wheel

following equation:

$$\eta_Z = \frac{P_{in} - P_{out}}{P_{in}} \tag{1}$$

The difference between the input power (P_{in}) and the output power (P_{out}) is called the total power loss (P_V), which is the sum of different sources of power loss. According to Höhn et al. [1] the gearbox power loss is due to gear load-dependent (P_{VZP}) and load-independent losses (P_{VZ0}), rolling bearing losses (P_{VL}), seal losses (P_{VD}) and auxiliary losses (P_{VX}) as resumed in Eq. (2) for a given load *i*.

$$P_V^i = P_{VZ0} + P_{VZP}^i + P_{VL}^i + P_{VD} \tag{2}$$

Note that P_{VZ0} and P_{VD} are, respectively, load-independent gear power loss and seal power loss. The seal losses are usually estimated using the Simrit equation [11]. The gear no-load losses (P_{VZ0}) are difficult to predict and models presented in the literature are only valid for a specific range of conditions, and for the moment, measuring gear no-load losses is the better solution to have a reliable power loss prediction [12–14].

The rolling bearing losses can be calculated with different models proposed in the literature. Martins et al. [8], Höhn et al. [1] and Durand de Gevigney et al. [15] used the Palmgren model [16]. Recently, Fernandes et al. [12] showed a good correlation between oil lubricated rolling bearing experiments and the SKF model [17]. Cousseau et al. [18] and Gonçalves et al. [19] also found good correlation between the SKF model and grease lubricated rolling bearings.

At each point along the path of contact, see Fig. 1, the load-dependent gear friction power loss is given by the following equation:

$$P_{VZP}(x) = F_N(x) \cdot \mu_Z(x) \cdot v_g(x) \tag{3}$$

Since the meshing starts at point A and ends at point E, the total friction power loss of the meshing gear is given by the following equation:

$$P_{VZP} = \int_A^E F_N(x) \cdot \mu_Z(x) \cdot v_g(x)\, dx \tag{4}$$

Eq. (4) is a general formulation for meshing gears friction power loss, making it necessary to know the product of force and sliding speed along the path of contact as well as the coefficient of

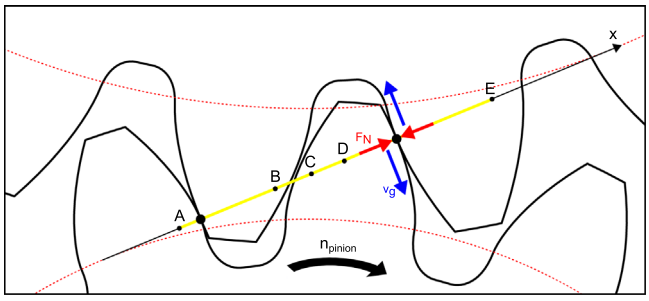

Fig. 1. Sliding speed and normal forces on the tooth contact.

friction at each point of the gear mesh. However, some simplifications are usual, and the coefficient of friction can be considered as a constant value along the path of contact (μ_{mZ}). For such case, Eq. (4) can be simplified in the form of the following equation:

$$P_{VZP} = \mu_{mZ} \cdot \frac{1}{p_b} \int_A^E F_N(x) \cdot v_g(x)\, dx \tag{5}$$

Then, it is known that the input power is given by the product of the transmitted load on the base circle (F_{bt}) and the tangential speed on the base circle (v_{tb}) as presented in the following equation:

$$P_{in} = F_{bt} \cdot v_{tb} \tag{6}$$

Multiplying and dividing Eq. (5) by the input power (Eq. (6)), P_{VZP} becomes the following equation:

$$P_{VZP} = \mu_{mZ} \cdot F_{bt} \cdot v_{tb} \cdot \frac{1}{p_b} \int_A^E \frac{F_N(x)}{F_{bt}} \cdot \frac{v_g(x)}{v_{tb}}\, dx \tag{7}$$

Eq. (7) is valid for spur gears. However, it can be generalised for helical gears, where the load and speed varies in the width direction. So, Eq. (8) is valid for all kind of gears with the contribution of the average coefficient of friction (μ_{mZ}), input power (P_{in}) and gear loss factor (H_{VL}) considering only the gear tooth geometry [20]. To calculate the local gear loss factor taking into account the elastic deformation of the tooth the method proposed by Marques et al. can be used [21].

$$P_{VZP} = \mu_{mZ} \cdot \underbrace{F_{bt} \cdot v_{tb}}_{P_{in}} \cdot \underbrace{\frac{1}{p_b} \int_0^b \int_A^E \frac{f_N(x,y)}{F_{bt}} \cdot \frac{v_g(x,y)}{v_{tb}}\, dx\, dy}_{H_{VL}} \tag{8}$$

3. Meshing gears coefficient of friction

The Stribeck work [22–24], published in 1902, showed the influence of the lubrication regime on the coefficient of friction of contacting bodies, as documented in Fig. 2. The Stribeck curve is still used today and shows how the coefficient of friction depends on the lubrication regime.

Gears very often operate under mixed film lubrication and a large number of empirical equations for the average coefficient of friction along the path of contact (mainly in mixed film regime) have been published in the literature [7,25–31]. Other authors [4,32–35] present equations for the coefficient of friction at each point along the path of contact, i.e. a local coefficient of friction.

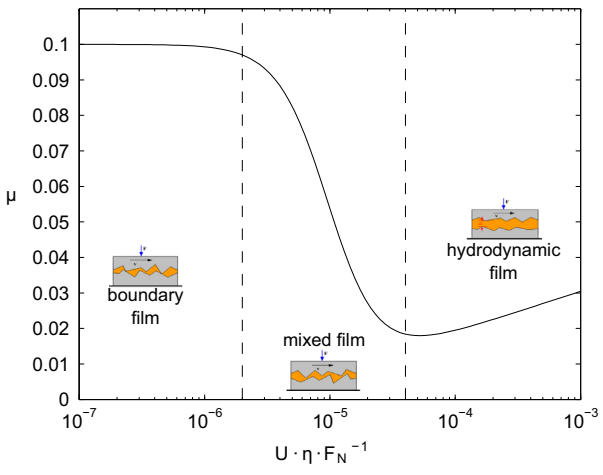

Fig. 2. Typical Stribeck curve: influence of the lubrication regime in the coefficient of friction.

Most of the formulas were obtained from the curve fitting of measured data collected in twin-disk tests. The equations that have been proposed are based on the following general equation:

$$\mu_{mZ} = f(\nu, \eta, v_g, v_r, \rho_{redC}, F_{bt}/b, p_0, R_a, \ldots) \tag{9}$$

Two groups of formulas can be found in the literature. The formulas that take into account the sliding speed, making it suitable for local coefficient of friction prediction. On the local gear coefficient of friction, Buckingham (1949) [4] was the first to introduce a coefficient of friction formula based on experimental results, proposing a coefficient of friction dependent on the oil, speed, load, material and surface finishing, but the formula only considered the sliding speed v_g. In the same group can be included the formulations of Misharin (1958) [32], O'Donoghue and Cameron (1966) [33], Drozdov and Gravikov [34] and Naruse (1984) [35].

In 1958, Ohlendorf [25] presented an equation which is applicable for the average coefficient of friction along the path of contact. On this type of equations are included the formulas developed by Eiselt (1966) [26], Matsumoto (1985 and 2014) [27,28], Michaelis (1986) [29], DIN 3990 (1987) [7], Schlenk (1994) [30] and Doleschel (2002) [31].

3.1. Average coefficient of friction

Schlenk [30] equation is more recent than DIN 3990 [7] and Michaelis [37] equations. Besides the influence of the viscosity of the lubricant, contact geometry and surface roughness, Schlenk included a parameter to take into account the oil formulation, the lubricant factor X_L. The lubricant factor allowed to distinguish different oils, and even more relevant to distinguish oils with the same viscosity properties but different base oil and additive packages. The work of Schlenk was recently included in the ISO standard 14179-2 [38] and his formula for the coefficient of friction between gear teeth is one of the most used. Schlenk's approach is presented in the following equation:

$$\mu_{mZ} = 0.048 \cdot \left(\frac{F_{bt}/b}{\nu_{\Sigma C} \cdot \rho_{redC}} \right)^{0.2} \cdot \eta^{-0.05} \cdot R_a^{0.25} \cdot X_L \tag{10}$$

Doleschel (2002) [31] defined the coefficient of friction in a gear mesh as a combination of the boundary coefficient of friction (μ_{bl}) and the full-film coefficient of friction (μ_{EHD}). The coefficient of friction in a gear mesh (μ_{mZ}) is then defined according to Eq. (11), where μ_{mZ} is the coefficient of friction in mixed film lubrication, μ_{bl} is the coefficient of friction under boundary film conditions and ξ is the portion of boundary friction (if $\xi = 1$, $\mu_{mZ} = \mu_{bl}$):

$$\mu_{mZ} = \xi \cdot \mu_{bl} + (1 - \xi) \cdot \mu_{EHD} \tag{11}$$

In the original work, the boundary film coefficient of friction and the full-film coefficient of friction were derived from experimental results in FZG tests [31].

The portion ξ of fluid and solid friction depends on the relative film thickness Λ in the contact and is given by the following equation [31]:

$$\xi = \begin{cases} 0.25 \cdot \Lambda^2 - \Lambda + 1, & \text{for} \Lambda < 2 \\ 0, & \text{for} \Lambda \geq 2 \end{cases} \tag{12}$$

The specific film thickness (or relative film thickness) is defined by the following equation [39]:

$$\Lambda = \frac{h_{0C}}{0.5 \cdot (R_{a1} + R_{a2})} \tag{13}$$

Recent findings by Matsumoto and Morikawa [28] showed that the equation proposed by Doleschel can correlate very well with experimental results. However, Matsumoto verified that the load sharing function should be calculated assuming R_z as the relevant surface parameter for the actual portion of solid/liquid coefficient

of friction instead of the average roughness (R_a), as proposed by Doleschel. Matsumoto's equation was based on the minimum film thickness proposed by Dowson and Higginson [40]. Matsumoto load sharing function is described by Eqs. (11), (14) and (15):

$$\xi = 0.5 \cdot \log D \tag{14}$$

$$D = \frac{R_{z1} + R_{z2}}{h_m} \tag{15}$$

Additionally, Matsumoto and Morikawa [28] also proposed a formula to use the average coefficient of friction equation to predict the local coefficient of friction along the path of contact as presented in the following equation:

$$\mu_Z(x) = \mu_{mZ} \cdot \beta_M \tag{16}$$

The value β_M is given in percentage (%) and $\beta_M = 0.1 \cdot SRR$, for a slide-to-roll ratio between 0 and 10%, while $\beta_M = 1$, for a slide-to-roll ratio higher than 10%.

Fig. 3 shows a comparison of the load sharing functions of Doleschel and Matsumoto. In general, Matsumoto equation predicts higher coefficient of friction (μ_{mZ}) than Doleschel equation for the same lubrication regime, assuming that the same μ_{bl} and μ_{EHD} values are used for both equations. Fig. 3 was obtained considering an ISO VG 32 mineral oil, without additives, at 100 °C, and a FZG type C spur gear (C14, see Appendix A) with the surface roughness presented in Table 1. The present example was used to compare both equations without any experimental validation.

Fig. 4 compares the coefficient of friction predicted by Schlenk, Doleschel and Matsumoto equations, and evaluates the influence of load, speed and temperature (viscosity) on the coefficient of friction predicted with each one of the equations. For this comparison the same ISO VG 32 mineral oil was considered. The values of μ_{bl}=0.09 and μ_{EHD}=0.0093 used in Eq. (11) are those determined by Matsumoto and Morikawa [28]. For Eq. (10) the value of X_L was set to X_L=1.

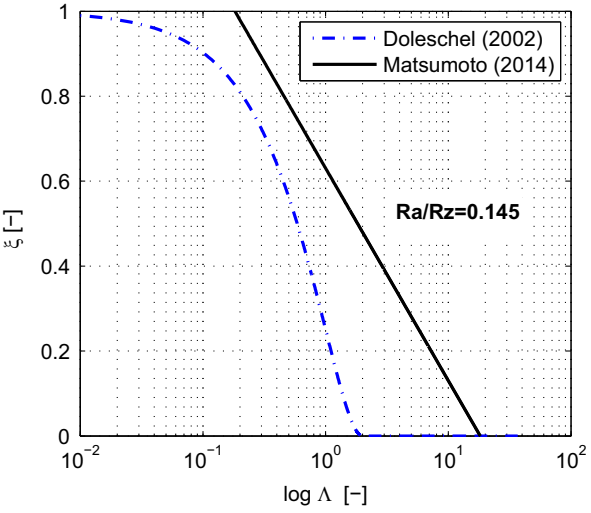

Fig. 3. Comparison of load sharing function of Doleschel and Matsumoto for an ISO VG 32 mineral oil without additives with a Type C gear.

Table 1
Tooth flank surface roughness of Type C spur gear.

Parameter	R_a (μm)	R_q (μm)	R_z (μm)	R_a/R_z (–)
Pinion	0.46	0.58	3.17	0.144
Wheel	0.61	0.78	4.21	0.146

Fig. 4a and b shows the behaviour of the equations at constant temperature, being clear that Doleschel and Matsumoto equations generated significantly different results considering the same reference values (μ_{bl}=0.09 and μ_{EHD}=0.0093). The influence of the boundary coefficient of friction on the average coefficient of friction is higher in Matsumoto's equation than in Doleschel's equation. In fact, Matsumoto's equation only achieves the full-film coefficient of friction when a specific lubricant film thickness is higher than 10, against Λ=2 in the case of Doleschel's equation. Schlenk's equation predicts similar values to those obtained with Doleschel's equation towards boundary lubrication. When film thickness increases, the coefficient of friction using Doleschel's equation drops suddenly due to a very low full-film coefficient of friction (μ_{EHD}), see Fig. 4a.

Matsumoto and Morikawa [28] presented μ_{bl} and μ_{EHD} values that take into account for the surface roughness. It is advised that boundary coefficient of friction (μ_{bl}) depends on the surface roughness, while full-film coefficient of friction (μ_{EHD}) is almost independent of surface finishing [28]. However, the influence of the operating temperature is not presented.

The results presented in Fig. 4a were predicted for 40 °C. It is clear that while μ_{bl} is almost constant no matter the operating temperature, the same is not true for μ_{EHD}. Fig. 5a shows the Stribeck curves of a mineral oil (MINR) and a PAO gear oil (PAOR) at different operating temperatures. Curve inflection means that full-film conditions are almost reached, being clear that temperature has a great impact on the full-film coefficient of friction as found in the literature [41,42].

The influence of the load on both Doleschel and Matsumoto formulations is almost the same since it is governed by the classical film thickness equations [40]. On the case of Schlenk's equation, the effect of load (torque) is more important as shown in Fig. 4b. The Schlenk equation is also less sensitive to the effect of the temperature (or viscosity) as presented in Fig. 4c.

According to ball-on-disc experimental results, presented as function of the modified Hersey parameter in Fig. 5b, for a given temperature and Hersey parameter, only a unique value of coefficient of friction may exist.

3.2. Local coefficient of friction

The equations discussed previously were determined assuming a constant coefficient of friction along the path of contact. However, that is a simplification of the problem and Bennedict and Kelley [43] introduced Eq. (17) that considers the variation of the sliding speed along the path of contact. However, the equation showed a singularity at the pitch point. This equation accounted also for rolling speed, dynamic viscosity and load, but disregarded the influence of the gear geometry (surface roughness and contact radius):

$$\mu_Z(x) = 0.0127 \cdot \log\left(f_N(x) \cdot \frac{29652}{\eta \cdot v_g(x) \cdot v_r(x)^2}\right) \tag{17}$$

Drozdov and Gavrikov [34] proposed Eq. (18) including the sliding speed effect, so it is suitable for local coefficient of friction prediction:

$$\mu_Z(x) = \left[0.8 \cdot \sqrt{\nu} \cdot v_g(x) + v_r(x) \cdot \phi + 13.4\right]^{-1} \tag{18}$$

The value of ϕ on Drozdov and Gravikov method is estimated with the following equation:

$$\phi = 0.47 - 1.3 \times 10^{-5} \cdot p_{max} - 4 \times 10^{-4} \cdot \nu \tag{19}$$

In 2005, Xu Hai [36] proposed a coefficient of friction based on results obtained with an EHL model (numerical results) that were validated with experimental traction curves. After validation, the

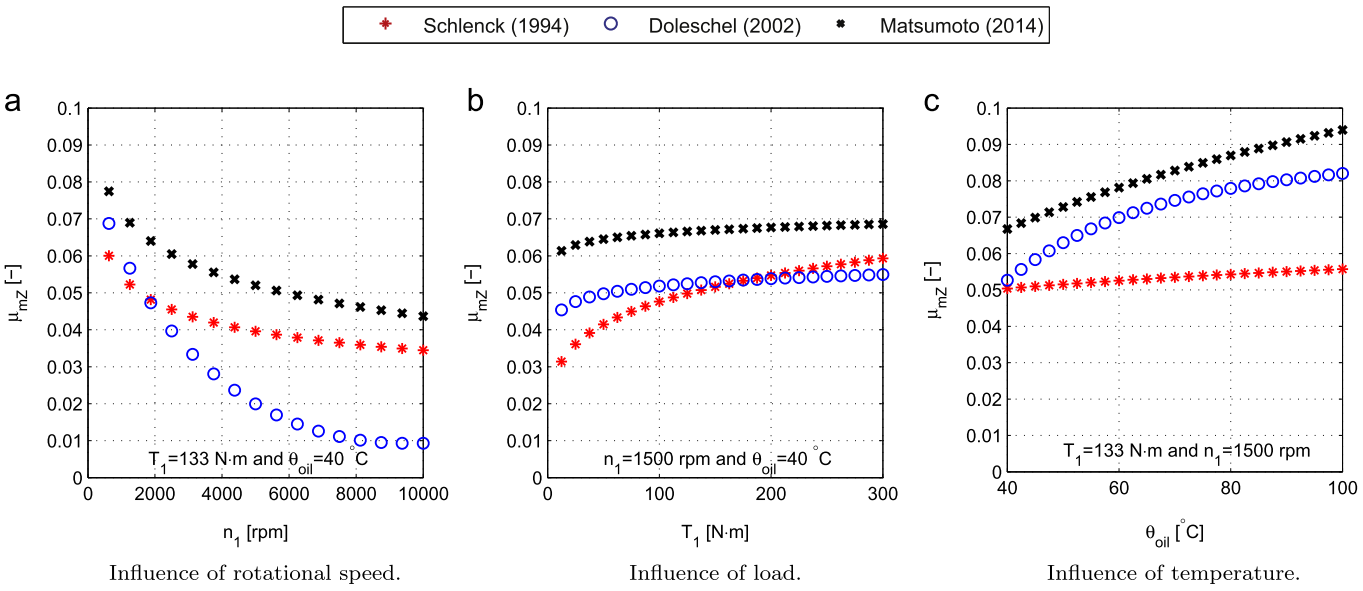

Fig. 4. Coefficient of friction for a Type C spur gear (C14) lubricated with an ISO VG 32 mineral oil without additives.

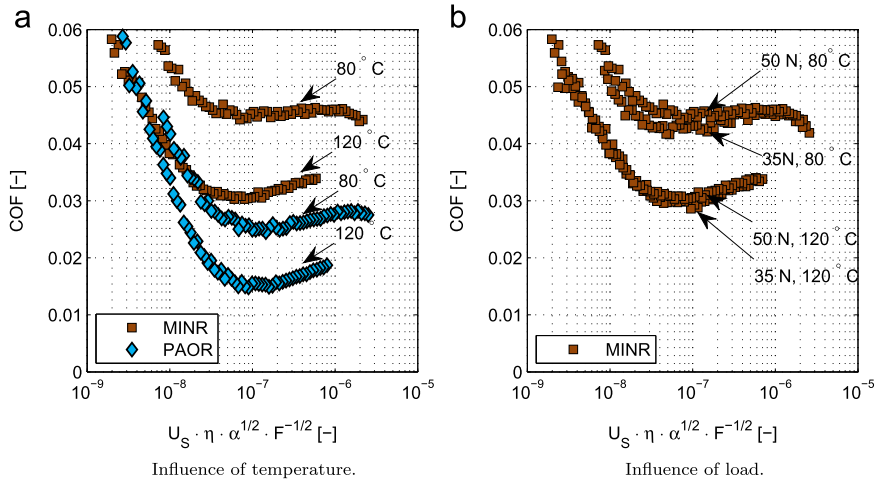

Fig. 5. Coefficient of friction measured with a ball-on-disc device [42].

model ran ≈ 10,000 times varying different operating conditions. These results were then fitted using a custom function based on key parameters, as represented in the following equations:

$$\mu_Z(x) = e^{f_{Xu}} \cdot p_h^{b2} \cdot |\mathrm{SRR}|^{b3} U_S^{b6} \cdot \eta^{b7} \cdot R_X^{b8} \quad (20)$$

$$f_{Xu} = b_1 + b_4 \cdot |\mathrm{SRR}| \cdot p_h \cdot \log_{10}(\eta) + b_5 \cdot e^{-|\mathrm{SRR}| \cdot p_h \cdot \log_{10}(\eta)} + b_9 \cdot e^{R_q} \quad (21)$$

The exponents for the Xu Hai equation are presented in Table 2.

Diez-Ibarbia et al. [44] proposed a modification for Schlenk equation in order to predict the local coefficient of friction. In the present work the Schlenk equation was modified as shown in Eq. (22). The modification takes into account that above 20% of slide-to-roll ratio the coefficient of friction is almost constant as proposed in the literature [1]. As the meshing process approaches the one to two teeth transition in a spur gear the SRR is close to 20%. The transition position can be approximated by $\frac{\epsilon_\alpha}{\epsilon_\alpha - 1}$ (valid for spur gears):

$$\mu_Z(x) = \mu_{mZ}(Schlenk) \cdot \tanh\left(\frac{\epsilon_\alpha}{\epsilon_\alpha - 1} \cdot |SRR(x)|\right) \quad (22)$$

Bennedict and Kelley [43], Drozdov and Gravikov [34] and Hai [36] equations were implemented for a spur gear (C40, see Appendix A) lubricated with a PAOR gear oil. Xu Hai equation was validated for a PAO so, it is suitable for this comparison. However, it should be noted that the coefficient of friction can be different from PAO to PAO according to the additive package used.

Table 2
Parameters for Xu Hai equation [36].

b_1	−8.916465
b_2	1.03303
b_3	1.036077
b_4	−0.354068
b_5	2.812084
b_6	−0.100601
b_7	0.752755
b_8	−0.390958
b_9	0.620305

The coefficient of friction behaviour of each formula can be observed in Fig. 6. It is clear that only Xu Hai equation follows the expected behaviour for the coefficient of friction along the path of contact as proposed in the literature [45,1].

The modified Schlenk and Xu Hai equations have a similar shape.

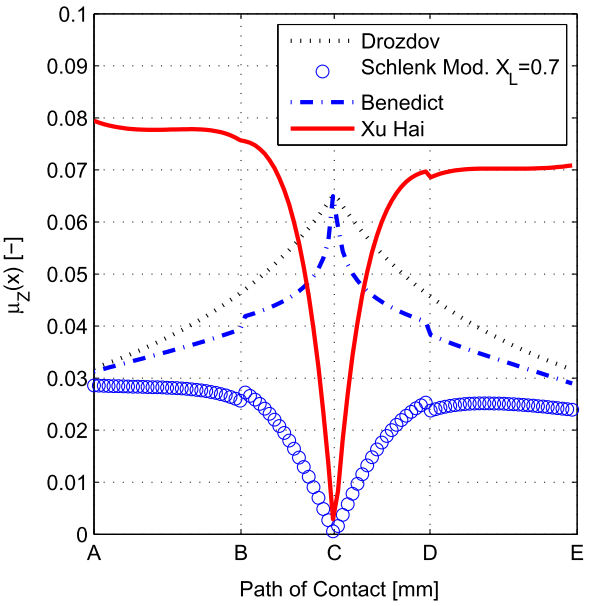

Fig. 6. Coefficient of friction along the path of contact for a spur gear (C40) lubricated with a PAOR gear oil at 1200 rpm and 199 Nm.

Table 3
Meshing gear power loss with different coefficient of friction formulas for a spur gear (C40) lubricated with a PAOR at 80 °C under 199 Nm.

Method	Speed					
	200		400		1200	
	P_{VZP} (W)	μ_{mZ}	P_{VZP} (W)	μ_{mZ}	P_{VZP} (W)	μ_{mZ}
Drozdov and Gavrikov	51.8	0.0659	92.3	0.0597	194.9	0.0441
Benedict and Kelley	53.4	0.0681	88.9	0.0567	183.2	0.0388
Xu et al.	68.1	0.0783	126.9	0.0731	341.0	0.0654
Schlenk Mod. (X_L=0.7)	28.7	0.0317	49.2	0.0276	118.6	0.0222
Schlenk (X_L=1)	49.6	0.0611	86.3	0.0532	207.9	0.0427
Schlenk (X_L=0.7)	34.7	0.0428	60.4	0.0373	145.6	0.0299
Experimental	34.6	0.0426	60.0	0.0370	138.9	0.0286

The coefficient of friction results for each equation is presented along the path of contact in Fig. 6. Solving Eq. (4) with the algorithm published in [20] for the load distribution along the path of contact, the meshing gears power loss (P_{VZP}) results were obtained for each formula and can be found in Table 3. It is clear that all the equations predicted a result significantly higher than the measured power loss. In that comparison, Schlenk equation was also used. Schlenk equation without lubricant factor calibration (X_L=1) presents similar results of those predicted with the other equations. It is important to note that two lubricants with same base oil and similar rheological properties can actually produce a different coefficient of friction depending on the complete formulation content, i.e. additives included as shown in [46]. For those cases it is almost impossible to use these kind of equations to characterize the coefficient of friction without including a lubricant factor that depends merely on the lubricant formulation (additives) as suggested by Schlenk [30].

Xu Hai equation produce a result much higher than that measured because the operating conditions are out of the boundaries advised by the author in terms of surface roughness $\sigma > 0.4$ [36].

4. Coefficient of friction derived from experimental results

In a previous work [47] the power loss in a FZG test rig assembled with C40 gears (see Appendix A), both in the driving and in the test gearboxes was measured. The oils considered were submitted to several tests in previous studies [12–14,48–53] and the main properties can be found in Appendix B.

The friction power loss generated by the meshing gears can be calculated for any load stage according to the following equation:

$$P_{VZP}^{EXP} = P_V^{EXP} - (P_{VZ0} + P_{VL} + P_{VD}) \tag{23}$$

The friction power loss P_{VZP} generated by the meshing gears (Eq. (23)) inside the gearbox can be used to calculate an experimental average coefficient of friction (μ_{mZ}^{EXP}) for all gear meshes of the gearbox. The average coefficient of friction μ_{mZ}^{EXP} can be calculated according to the following equation:

$$\mu_{mZ}^{EXP} = \frac{P_{VZP}^{EXP}}{P_{in} \cdot H_{VL}} = \frac{P_V^{EXP} - (P_{VZ0} + P_{VL} + P_{VD})}{P_{in} \cdot H_{VL}} \tag{24}$$

In previous works [12,13] a method to quantify the no-load gear losses, rolling bearing and seal power losses was presented.

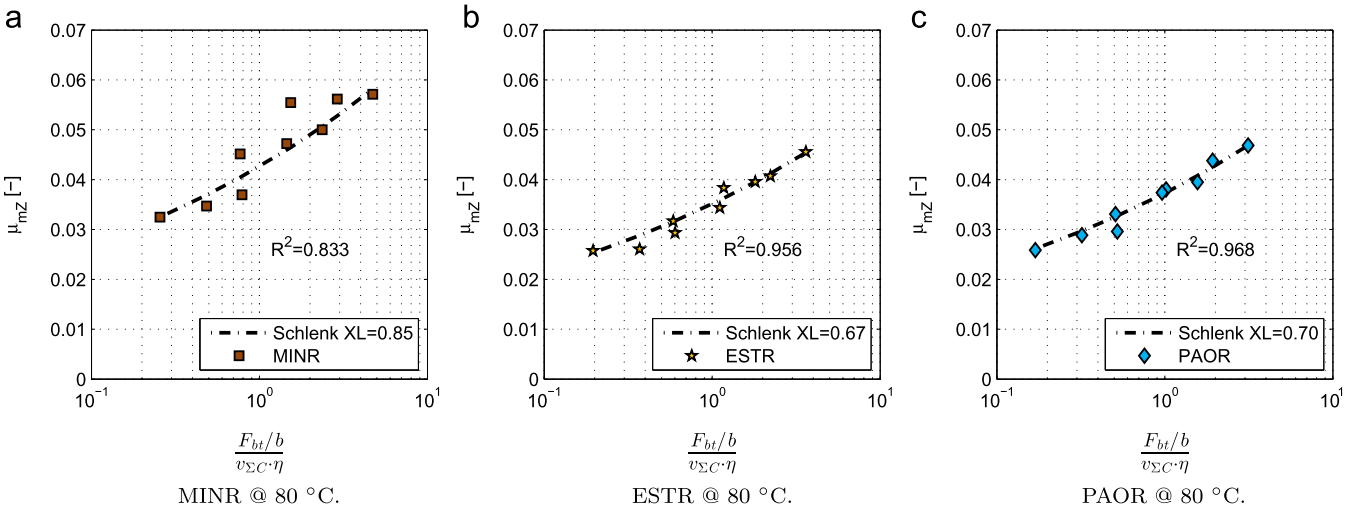

Fig. 7. Experimental coefficient of friction of spur gears (C40) and Schlenk coefficient of friction with adjusted X_L vs. hydraulic parameter (H_p) [47].

The gear results are usually presented in the literature as a function of the hydraulic parameter concept, given by the following equation [54]:

$$H_p = \frac{F_{bt}/b}{v_{\Sigma C} \cdot \eta} \tag{25}$$

The experimental coefficient of friction determined based on experiments in a previous work [47] is presented in Fig. 7 as a function of the hydraulic parameter (H_p). The Schlenk equation is proportional to the hydraulic parameter, indicating its interdependence. The results show that ESTR and PAOR follow reasonably well the Schlenk equation and are more or less proportional to the hydraulic parameter. However, MINR clearly has a completely different behaviour despite the good numerical correlation observed between experiments and Schlenk formula (correlation factor, R^2=0.833).

5. Proposal of a new load sharing function to predict the coefficient of friction under mixed lubrication regime

The pressure–viscosity coefficient can be related to the limiting shear stress, as proposed by several authors [55–58]. So, selecting a lubricant with higher pressure–viscosity coefficient can aid to form a thicker film but will promote a higher limiting shear stress promoting higher coefficient of friction, at least under full-film lubrication [59]. Then, it is of great interest to include the pressure–viscosity coefficient as a significant property when studying the coefficient of friction of lubricating contacts.

Brandão et al. [59] performed several traction measurements on a ball-on-disc for gear oils and proposed a modified Hersey parameter taking into account the pressure–viscosity coefficient of the lubricants. The results obtained indicate that under mixed film lubrication regime, the coefficient of friction decreases with increasing values of the modified Hersey parameter (S_p). Since the results were presented in a logarithmic scale, the relation between the coefficient of friction and S_p was almost linear. Introducing the pressure–viscosity on the new parameter (S_p), the friction behaviour of lubricants with the same operating viscosity is clearly distinguished for different base oils as shown in Fig. 8b. Different base oils (mineral, PAO or ester) imply different pressure–viscosity coefficient.

The traction coefficient measurements presented in a previous work [42] also showed a linear dependence of the traction coefficient with S_p parameter. Thus, the experimental average coefficient of friction, based on gear experiments, can also be plotted against the modified Hersey parameter.

The modified Hersey parameter, Eq. (26), was adapted to gears making the following assumptions:

- Velocity U_S, is equal to the sum of the velocities at the pitch point, i.e. $U_S = v_{\Sigma C}$.
- The load F is equal to the tangential force on the base plane, i.e. $F = F_{bt}$:

$$S_p = \frac{U_S \cdot \eta \cdot \alpha^{1/2}}{F^{1/2}} \tag{26}$$

Thus,

$$S_p^{gear} = \frac{v_{\Sigma C} \cdot \eta \cdot \alpha^{1/2}}{F_{bt}^{1/2}} \tag{27}$$

Figs. 9a–c indicate a linear trend (on a log scale) for the variation of the average coefficient of friction with S_p parameter.

The results presented in Fig. 9 show a linear trend when presented against the modified Hersey parameter under mixed film lubrication regime.

A direct comparison between the hydraulic parameter and the modified Hersey parameter shows two main differences: different influence of load and inclusion of pressure-viscosity on modified Hersey parameter, particularly useful to make distinctions between lubricants with similar operating viscosities.

The current trend on literature is to use the film thickness ratio (Λ) to describe the dependence of the coefficient of friction on the lubrication regime, as presented by Doleschel [31] and Matsumoto and Morikawa [28]. However, this type of representation (μ_{mZ} vs. Λ) can show some incoherences, as presented in Fig. 8a. Despite the format of the load sharing function (ξ) used and the given set of μ_{bl} and μ_{EHD} values, only one coefficient of friction is achieved for each Λ ratio, which based on experiments it is not true. In fact, for the same Λ ratio quite different coefficient of friction values may exist depending, mainly, on the full-film coefficient of friction (μ_{EHD}) that is strongly dependent on operating temperature and slightly on the load. To correlate the experimental coefficient of friction with values predicted using the methods proposed in the literature, reference values of μ_{bl} and μ_{EHD} are needed for each applied load or each operating temperature.

Using a load sharing function (ξ) based on a modified Hersey parameter, for each value of coefficient of friction, only one

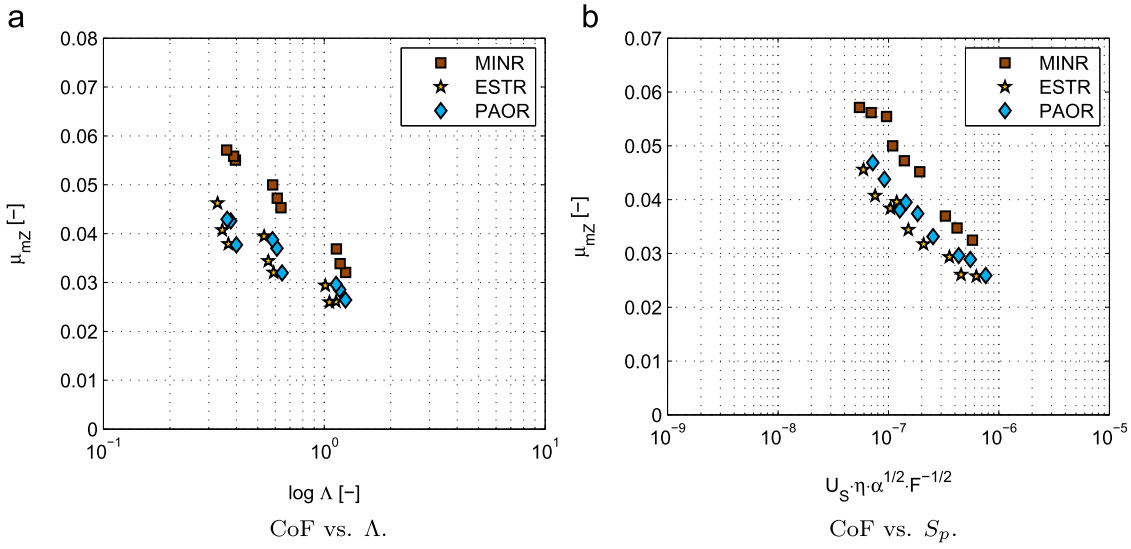

Fig. 8. Coefficient of friction vs. different parameters representing the lubrication condition.

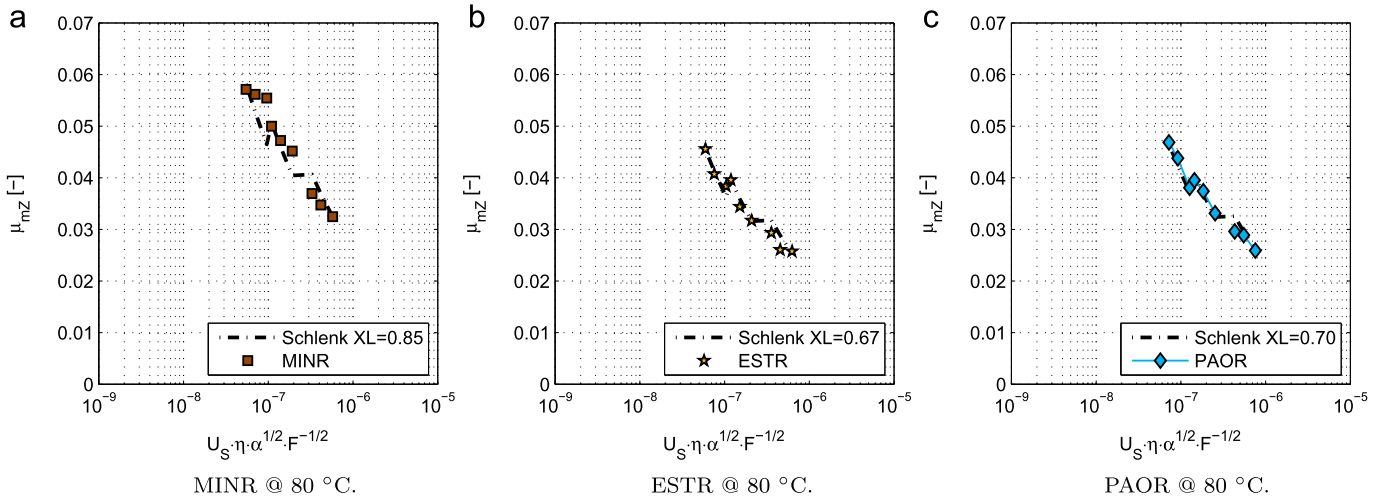

Fig. 9. Experimental coefficient of friction of spur gears (C40) and Schlenk coefficient of friction with adjusted X_L vs. modified Hersey parameter (S_p).

modified Hersey parameter value exist, as shown in Fig. 8b, that only depends on lubricant formulation.

5.1. Load sharing function

A logarithmic line with the topology of Eq. (28) can present the influence of S_p on the coefficient of friction, as shown by experiments:

$$y = m \cdot \log_{10}(x) + b \tag{28}$$

Based on the equation, the load sharing function (ξ) can be written as follows:

$$\xi = m \cdot \log_{10}(S_p) + b \tag{29}$$

The modified Hersey parameter (S_p) only takes into account the lubrication conditions and does not consider the influence of the contact geometry. The modified Hersey parameter can only describe the influence of the load (F), velocity (U_S), dynamic viscosity (η) and pressure–viscosity coefficient (α). While load, speed and oil properties are important data to study coefficient of friction, the contact geometry is also important. So, a geometric parameter of the contact must be included in the equation.

5.2. Gear geometric parameter

To include the influence of the gear tooth geometry (macro and micro geometry) on the load sharing function, the geometric parameters, such as the surface finishing (R_a), the average face width contact ($\epsilon_\alpha \cdot b \cos\beta_b$) and the equivalent radius of contact (ρ_{redC}), will be considered to create a dimensionless geometric parameter for the gear in the format of the following equation:

$$S_g = \frac{R_a^{A_g}}{\rho_{redC}^{B_g} \cdot (\epsilon_\alpha \cdot b \cos\beta_b)^{C_g}} \tag{30}$$

The basic principle is that a geometric parameter should be combined with the modified Hersey parameter, aiming to include the contact geometry. A lower geometric parameter value (S_g) means that we get closer to full-film lubrication conditions. It happens when surface roughness (R_a) is decreased or curvature radius (ρ_{redC}) and face width (b) are increased. Under this assumption, the load sharing function can be the following equation:

$$\xi = m \cdot \log_{10}(S_p \times S_g) + b \tag{31}$$

The main objective is to find a dimensionless geometric parameter (S_g). To compute the different exponents the following hypothesis were assumed:

- The influence of roughness is kept the same as mentioned in early studies published by Höhn et al. [1], i.e. $[1 + m \cdot \log_{10}(\mathrm{Ra})] \approx \mathrm{Ra}^{0.25}$.
- The parameter is valid for mixed lubrication conditions.
- The average roughness range tested is 0.3–0.7 μm.
- Average length of contact along the path of contact of the meshing gears ($\epsilon_\alpha \cdot b \cos\beta_b$) has the same exponent of equivalent radius on pitch point (ρ_{redC}).
- The parameter is dimensionless.

Since gear geometry is a constant for macro and micro-geometry combination, such hypothesis was taken assuming that the parameter can be calibrated in a future work keeping all the data here presented valid.

The Buckingham theorem gives the following equation:

$$A_g = B_g \cdot C_g \tag{32}$$

At same time, it was considered that $B_g = C_g$, which allows to determine each exponent in the following equation:

$$B_g = C_g = \frac{1}{2} \cdot A_g \tag{33}$$

Finally, S_g and S_p are given by Eqs. (34) and (35), respectively with all quantities expressed in SI units:

$$S_g = \frac{R_a}{(\rho_{redC} \cdot \epsilon_\alpha \cdot b \cos\beta_b)^{1/2}} \tag{34}$$

$$S_p = \frac{U_S \cdot \eta \cdot \alpha^{1/2}}{F^{1/2}} \tag{35}$$

The load sharing function is given by Eq. (36). The parameter $S_p \times S_g$ was multiplied by 10^9 based on the evidence that for values of $S_p \times S_g \times 10^9 < 1$, the gear operates under boundary lubrication. Usually, mixed lubrication condition may exist, between $S_p \times S_g = 1 \times 10^{-12}$ and $S_p \times S_g = 10^{-10}$, as shown in Appendix C.

$$\xi = 0.5 \times \log_{10}\left(S_p \times S_g \times 10^9\right) \tag{36}$$

The coefficient of friction, based on the presented sharing function, should be estimated as shown in the following equation:

$$\mu_{mZ} = (1 - \xi) \cdot \mu_{bl} + \xi \cdot \mu_{EHD} \tag{37}$$

In order to verify each sharing function, and since no measurements of reference values of μ_{bl} and μ_{EHD} exist to predict the

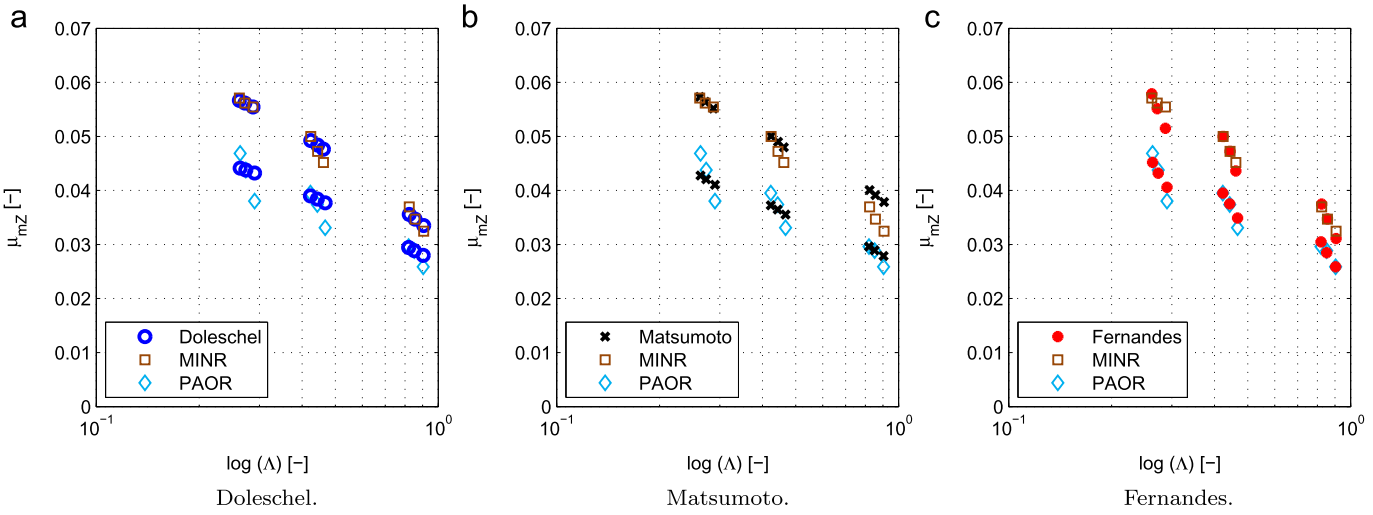

Fig. 10. Experimental coefficient of friction of spur gears (C40) and sharing function formulas prediction with numerical fit (Table 4).

Table 4
Numerical reference values (μ_{bl} and μ_{EHD}) and correlation (R^2).

Oil	Property	Doleschel	Matsumoto	Fernandes
MINR	μ_{bl}	0.071	0.073	0.065
	μ_{EHD}	0.027	0.001	0.012
	R^2	0.985	0.993	0.977
PAOR	μ_{bl}	0.054	0.056	0.051
	μ_{EHD}	0.024	0.000	0.013
	R^2	0.872	0.908	0.969

experimental results presented in Section 4, a numerical procedure was used. Based on the experimental results, each sharing function was used to verify if the behaviour of the experimental results is well presented. To do that, the reference values were determined numerically. The results are found in Table 4 and Fig. 10.

No significant differences were found for the correlation achieved with each formula. However, it is clear that the numerical value of full-film coefficient of friction is quite different depending on the formula used. Is is clear that the new sharing function follows slightly better the behaviour of the experimental results.

6. Simplified coefficient of friction equation

Assuming the linear variation of the coefficient of friction with S_p, given by the following equation:

$$\mu_{mZ} \propto m \cdot \log\left(S_p \times S_g\right) + b \tag{38}$$

The logarithmic function can be approximated by the following equation:

$$\mu_{mZ} \propto A_p \cdot \left(S_p \times S_g\right)^{B_p} \tag{39}$$

The lubricant factor X_L was introduced by Schlenk to account for the influence of each oil formulation and in a previous work [13] it was determined for different wind turbine gear oils. It is of great interest to keep the same parameter on the new equation aiming to clearly make a distinction between different base oils and additive packages.

Combining the dimensionless parameters, S_p and S_g, the following system of Eqs. (40) will be adjusted to the experimental results presented in Fig. 9 to determine A_p and B_p:

$$\mu_{mZ} = A_p \cdot \left(\frac{U_S \cdot \eta \cdot \alpha^{1/2}}{F^{1/2}}\right)^{-B_p} \cdot S_g^{B_p} \cdot X_L \tag{40}$$

In order to fit experimental results, A_p and B_p are constant values no matter the oil formulation used. The oil formulation is accounted by in the lubricant factor X_L previously determined using Schlenk's equation. The minimisation process give the following values: $A_p = 0.014$ and $B_p = 0.25$. So, the final equation takes the form (41),

$$\mu_{mZ} = 0.014 \cdot \left(\frac{1}{S_p}\right)^{1/4} \cdot S_g^{1/4} \cdot X_L \tag{41}$$

The prediction of the coefficient of friction using the new equation is presented in Fig. 11 for MINR, ESTR and PAOR. It is interesting to verify that the new equation follows rather well the behaviour of the experimental coefficient of friction results.

The new equation includes the influence of the pressure–viscosity coefficient, which produces a very interesting effect under constant temperature and operating viscosity: for each rotational speed the slope of the equation will be different (for example: ESTR and PAOR). The highest the pressure–viscosity the lowest is the slope, for the same operating speed. It makes sense, since for the same operating condition and similar operating viscosity, it is expected that the oil with the highest pressure–viscosity generates slightly higher film thickness, and consequently the coefficient of friction is less influenced by the load, but not necessarily a lower coefficient of friction is produced [58].

The equation was applied to helical gear results published in [13] for a H501 (see Appendix A) lubricated with a MINR oil (see Appendix B). The results are presented in Fig. 12a. The new formulation follows the experimental results behaviour, but it is clear that some additional work is needed to better calibrate the gear geometry parameter (S_g).

The accuracy of the torque measuring system on the FZG machine is ± 0.1 N m [47], which is independent of the gear tooth geometry.

The average coefficient of friction based on experimental results (Eq. (42)) is then more sensible to the accuracy of the measuring system for "low loss" gears with low gear loss factor H_{VL} such as gear H951 (see Table A1, Appendix A):

$$\mu_{mZ}^{EXP} = \frac{P_{VZP}^{EXP}}{P_{in} \cdot H_{VL}} \tag{42}$$

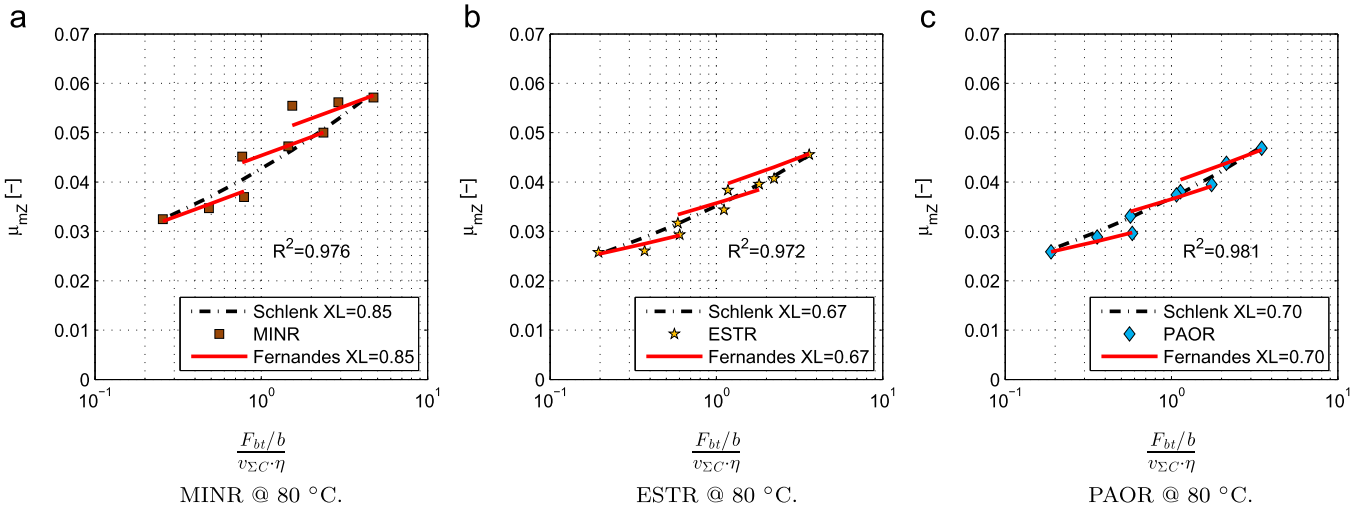

Fig. 11. Coefficient of friction determined based on experimental results of spur gears (C40) vs. Schlenk equation adjusted and Fernandes equation, for MINR as function of hydraulic parameter.

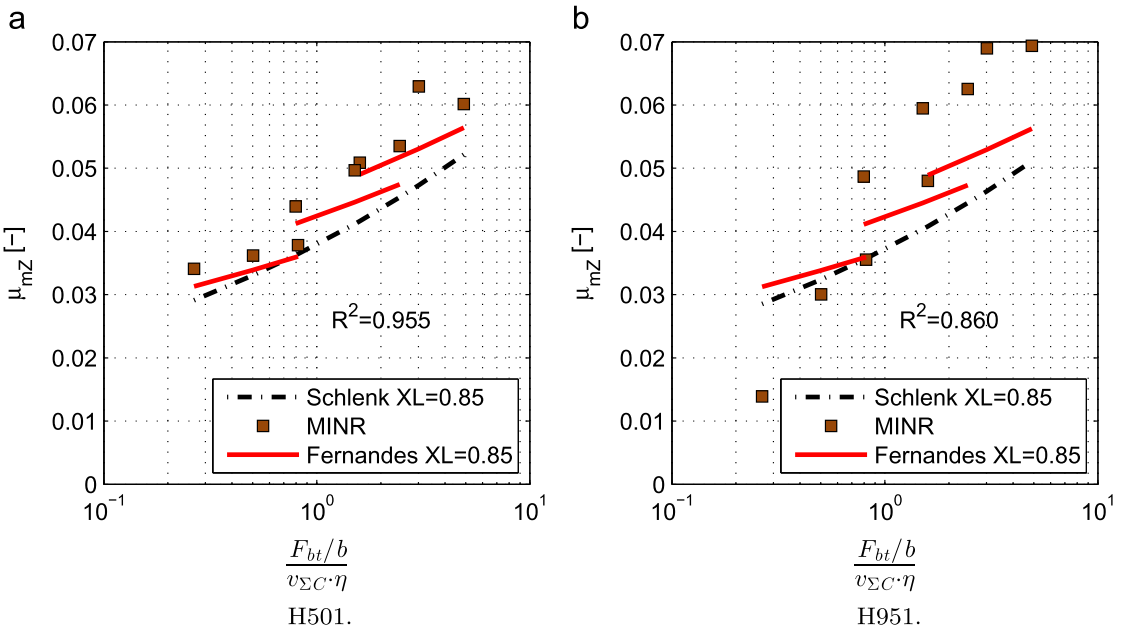

Fig. 12. Coefficient of friction determined based on experimental results of helical gears (H501 and H951) vs. Schlenk equation adjusted and Fernandes equation, for MINR as function of hydraulic parameter.

From the results presented in Fig. 12b it can be clearly stated that it is quite hard to extract a coefficient of friction from H951 gear tooth geometry results mainly because of its very low H_{VL}. However, the correlation is still good for all the gear tooth geometries considered. In order to have more confidence in the results a less efficient and simpler gear tooth geometry like the C40 gear tooth geometry was used aiming to accurately tune the new coefficient of friction equation. Once a proper lubricant factor X_L is found, the equation can be used to evaluate the power loss both in spur and helical gears.

In order to compare the prediction of the coefficient of friction using both equations, Schlenk and the new formula (41), Fig. 13 shows the predictions for twin-disc tests published by Höhn et al., performed at 90 °C with a SRR=10% and a sum of the velocities from 1 to 16 m/s. This set of results was selected because were used to calibrate Schlenk's equation. Three lubricants with mineral base oil, without additives, were considered: FVA2 ISO VG 32 ($\nu_{90}=4.4$ mm^2/s), FVA 3 ISO VG 100 ($\nu_{90}=14.5$ mm^2/s) and FVA4 ISO VG 460 ($\nu_{90}=46$ mm^2/s). According to Höhn et al. [1], slide-to-roll ratios above 10% do not influence the coefficient of friction. For this situation, the lubricant factor X_L is set equal to 1.

Fig. 13 clearly shows that the new formula for the coefficient of friction (41) fits very well all experimental results within a mixed lubrication condition.

Since the proposed equation is suitable for the average coefficient of friction prediction, it was compared with Schlenk, Doleschel and Matsumoto formulas in Fig. 14. The influence of load, speed and viscosity are quite different on the new equation. The equation showed a similar dependency on the speed of that found for Schlenk equation. The load influence quantified by the equation is similar to that presented by Doleschel and Matsumoto. The viscosity influence is similar to the one found on Matsumoto formula.

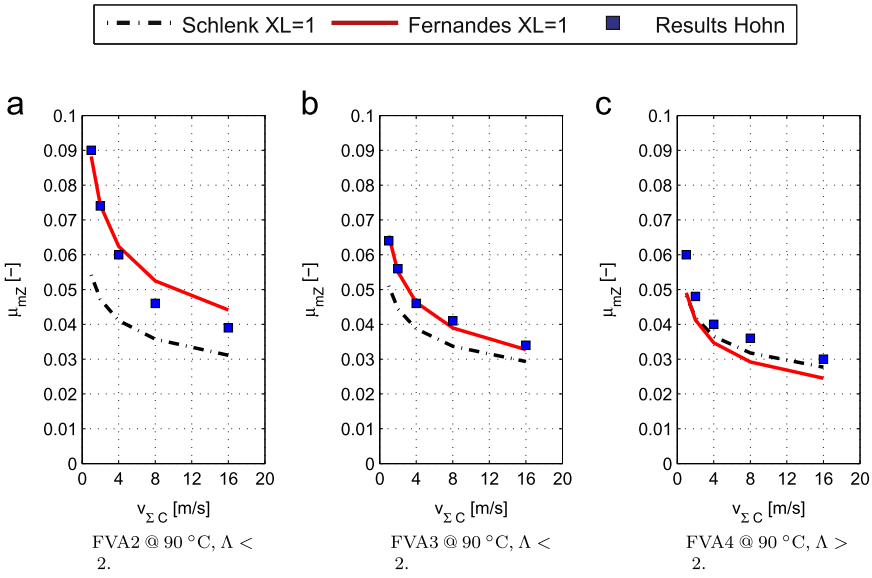

Fig. 13. Fernandes and Schlenk formulas predicting the twin-disc results published by Höhn et al. [1].

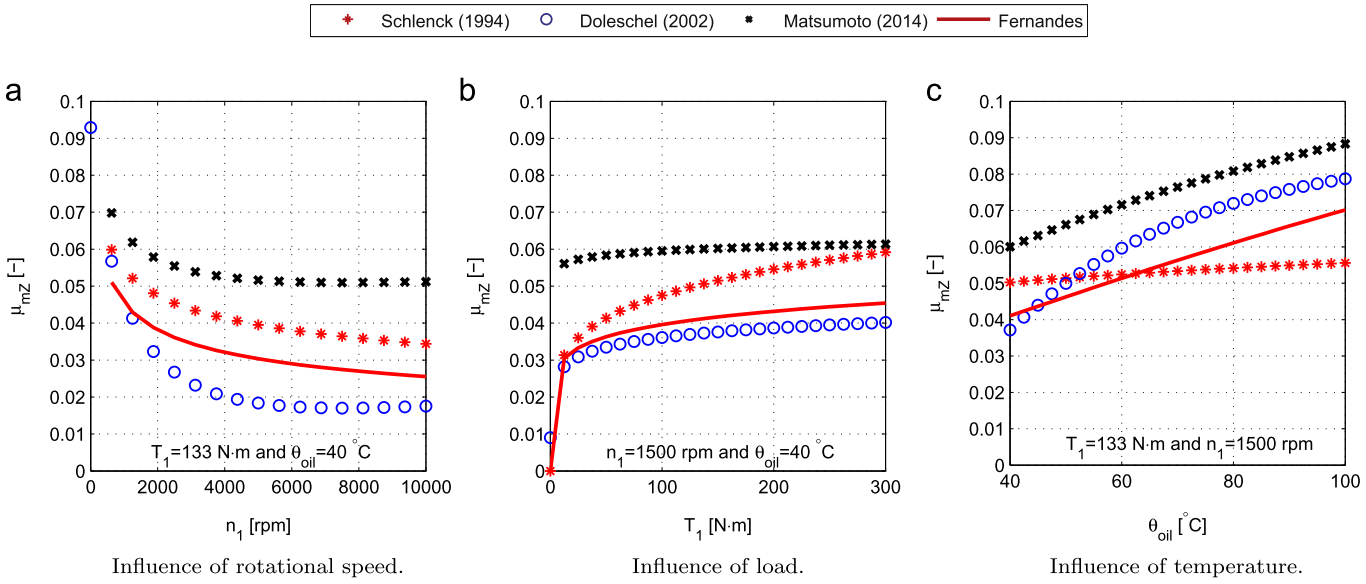

Fig. 14. Coefficient of friction for a Type C spur gear (C14) lubricated with an ISO VG 32 mineral oil without additives.

7. Conclusions

Different equations presented in the literature for average and local coefficient of friction were revisited. These formulas were used to estimate the average coefficient of friction between meshing teeth, and the results were compared against some experimental values. A new average coefficient of friction equation is proposed, taking into consideration the influence of oil pressure–viscosity coefficient.

Based on gear experimental results a linear correlation between coefficient of friction results and a modified Hersey parameter that accounts for pressure–viscosity parameter was observed. The linear behaviour was also observed for other types of contacts like ball-on-disc. Furthermore, there are some additional evidences in the literature that the pressure–viscosity coefficient is linearly correlated with the coefficient of friction.

The new formulation proposed was built around the modified Hersey parameter which accounts for load, speed, viscosity and pressure–viscosity effects. It correlates quite well with the experimental results, both those specifically performed to validate the new equation as well as other results found in the literature.

Acknowledgements

The authors gratefully acknowledge the funding supported by National Funds through Fundação para a Ciência e a Tecnologia (FCT), under the Project EXCL/SEM-PRO/0103/2012; COMPETE and National Funds through Fundação para a Ciência e a Tecnologia (FCT), under the Project Incentivo/EME/LA0022/2014; Quadro de Referência Estratégico Nacional (QREN), through Fundo Europeu de Desenvolvimento Regional (FEDER), under the Project NORTE-07-0124-FEDER-000009 – Applied Mechanics and Product Development; without whom this work would not be possible.

Table A1
Geometry of the gears.

Property	Gear type							
	C14		C40		H501		H951	
	Pinion	Wheel	Pinion	Wheel	Pinion	Wheel	Pinion	Wheel
Number of teeth	16	24	16	24	20	30	38	57
Module (mm)	4.5		4.5		3.5		1.75	
Centre distance (mm)	91.5				91.5			
Pressure angle (deg)	20				20			
Helix angle (deg)	–				15			
Face width (mm)	14		40		23		23	
Addendum modification x_z (–)	+0.1817	+0.1715	+0.1817	+0.1715	+0.1809	+0.0891	+1.6915	+2.0003
Addendum diameter (mm)	82.64	118.54	82.64	118.54	80.67	116.27	76.23	111.73
Transverse contact ratio ϵ_α (–)	1.44		1.44		1.46		0.93	
Overlap contact ratio ϵ_β (–)	–		–		0.54		1.08	
Ra (μm)	≈0.5		≈0.7		≈0.35		≈0.35	
H_{VL} (–)	0.1949		0.1949		0.1869		0.0689	
Material	16MnCr5							

Appendix A. Geometric properties of the gears considered

In previous works the torque loss of different gear tooth geometries and different wind turbine gear oils was measured allowing to calibrate a power loss model. Torque loss results of C40 spur gears were presented in [47], C14 spur gears in [60] and H501 helical gears in [13].

Table A1 displays the main geometric properties of the gears.

Appendix B. Physical and chemical characterisation of fully formulated wind turbine gear oils

B.1. Rheology

Tests at 40, 70 and 100 °C, using an Engler viscometer, were performed in order to measure the kinematic viscosity of all the wind turbine gear oils. The kinematic viscosity measurements are presented in Table B1 and all the oils are in the range acceptable for an ISO VG 320 grade oil 320 ± 32 cSt.

Using ASTM D341 [61] Eq. (B.1) it was possible to calculate the ASTM constants m_A and n_A keeping the constant value of a_A=0.7 for all the oils:

$$\log\ \log(\nu + a_A) = n_A - m_A \cdot \log(T) \tag{B.1}$$

The density was measured with an Anton Par densimeter, a portable unit. The range of temperature available goes from 15 up to 40 °C which is enough to know the density of a fluid under ambient temperature conditions. It is known that the density depends on the temperature [40]. However, the influence of the pressure on the density is much more important than the influence of the temperature.

The density was measured at 15 °C, which is the reference temperature (θ_0) and the values are presented in Table B1. Additional measurements were performed up to the limit temperature of the densimeter. The values measured were used to evaluate the thermal expansion coefficient (α_t), according to Eq. (B.2), also presented in Table B1:

$$\rho = \rho_0 + \alpha_t \cdot \rho_0 (\theta_0 - \theta) \tag{B.2}$$

B.2. Pressure–viscosity

Under elastohydrodynamic lubrication conditions, the formation of the lubricating film is strongly dependent on the pressure-viscosity behaviour of a lubricating oil, as shown in the literature [40].

The kinematic viscosities measured and presented in Table B1 may be used to determine the pressure–viscosity coefficient using Gold's Eq. (B.3). The pressure–viscosity coefficient can be determined for a pressure of 0.2 GPa, usual value of the pressure in the inlet zone of the contact, where the film formation occurs [40]. Depending on the base oil, the s and t values are provided by Gold

Table B1
Density (ρ), thermal expansion coefficient (α_t), kinematic viscosity (ν), ASTM constants (m_A, n_A) and viscosity index (VI) for the wind turbine gear oils.

Parameter	Unit	MINR	ESTR	PAOR
ρ@ 15 °C	g/cm^3	0.902	0.915	0.859
$\alpha_t \times 10^{-4}$	–	5.8	8.1	5.5
ν @ 40 °C	cSt	319.2	302.9	313.5
ν @ 70 °C	cSt	65.8	77.5	85.0
ν @ 100 °C	cSt	22.3	34.9	33.3
m_A	–	9.066	7.582	7.351
n_A	–	3.473	2.880	2.787
VI	–	85	165	153

Table B2
Constants of Gold equation at 0.2 GPa and pressure–viscosity coefficient at 80 °C for each wind turbine gear oil.

Parameter	MINR	ESTR	PAOR
s	0.9904	0.6605	0.7382
t	0.1390	0.1360	0.1335
$\alpha \times 10^8$ (1/Pa)	1.677	1.158	1.279

Table B3
ICP analysis of the wind turbine gear oils.

Parameter	Unit	MINR	ESTR	PAOR
Sulphur (S)	ppm	11,200	406	5020
Phosphorus (P)	ppm	354.3	226.2	415.9
Boron (B)	ppm	22.3	1.7	28.4
Calcium (Ca)	ppm	2.5	14.4	0.5
Zinc (Zn)	ppm	0.9	6.6	3.5
Magnesium (Mg)	ppm	0.9	1.3	0.5

et al. [62]:

$$\alpha = s \cdot \nu^t \times 10^{-8} \quad \text{(B.3)}$$

The pressure–viscosity coefficient can be calculated with some degree of confidence for MINR (mineral naphtenic), ESTR (ester) and PAOR (polyalphaolephin) using Eq. (B.3).

With the "Gold" constants s and t previously published [62] (see Table B2), the pressure–viscosity coefficients can be calculated at different temperatures. Table B2 shows the α values for each wind turbine gear oil at 80 °C. It is possible to verify that the oils have the following behaviour: $\alpha_{MINR} > \alpha_{PAOR} > \alpha_{ESTR}$.

Mia et al. [63] determined the pressure–viscosity coefficient from high-pressure rheology for a mineral oil and different PAO wind turbine oil formulations. The values found are slightly lower than those calculated through Gold's equation. Mia et al. values are 15% lower in the case of mineral oil and 9% lower in the case of the PAO.

B.3. Inductively coupled plasma atomic emission spectrometry (ICP-AES)

Atomic Emission Spectrometry was performed for all wind turbine gear oils, and the results are presented in Table B3. The elements identified are: Zinc, Magnesium, Phosphorus, Calcium, Boron and Sulphur. Using only ICP, it is almost impossible to understand which particular compounds are present in the fully formulated products.

The sulphur is a constituent of the mineral based oils, but the concentration is not greater than 300 ppm. The concentration of sulphur in MINR and PAOR is very high, which can be explained by the presence of EP additives that are sulphur and phosphorous compounds. It is documented that EP oils usually have values of phosphorus greater than 200 ppm and boron can reach 25 ppm, which is verified for MINR and PAOR. The inclusion of EP additives is advised by the manufacturers of the referenced products.

ESTR is a biodegradable product, thus showing much lower sulphur concentration, as expected for biodegradable fluids with low toxicity.

Appendix C. Load sharing functions

In order to study the consistency of each formula behaviour, the geometrical properties as well as the operating conditions were modified in the range presented in Table C1.

A numerical combination of the geometrical properties and operating conditions (Table C1) was calculated. It is clear that a given range of Λ ratio is comprised for a certain range of $S_p \times S_g$ parameter, supporting its relationship as presented in Fig. C1. Each vector has three elements equally spaced from lower up to upper values.

In Fig. C2 is presented each load sharing function for the combination of each vector from Table C1. For this case each vector has two elements (lower and upper values, respectively).

Table C1
Geometrical properties and operating conditions range.

Property	Unit	Lower value	Upper value
R_a	μm	0.181	0.906
R_z	μm	1.845	9.225
b	mm	10	50
R_X	mm	4.2	12.57
η	m Pa s	3.9	97.5
α	Pa^{-1}	0.839×10^{-8}	2.096×10^{-8}
U_S	m/s	0.432	8.63
F_{bn}	N	2000	8000
S_p [a]	–	1.7×10^{-9}	2.7×10^{-6}
S_g [a]	–	7.2×10^{-6}	1.4×10^{-4}

[a] Resulting from combination of values above.

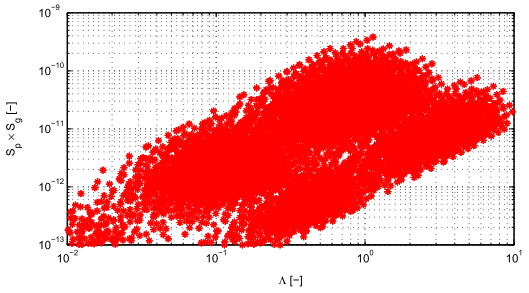

Fig. C1. Relation between $S_p \times S_g$ and Λ ratio.

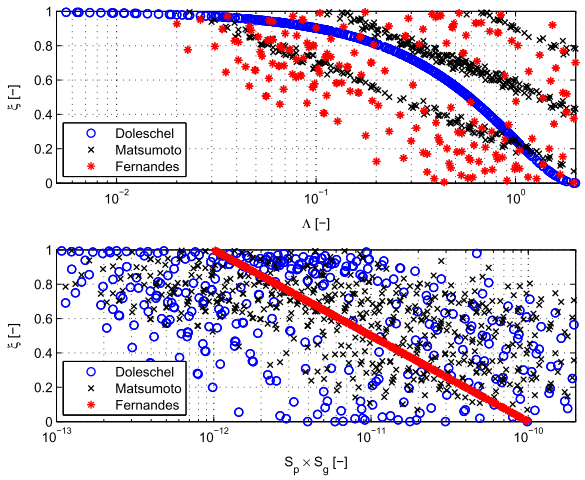

Fig. C2. Different load sharing functions behaviour vs. Λ ratio and modified Hersey parameter.

References

[1] Höhn B-R, Michaelis K, Vollmer T. Thermal rating of gear drives: balance between power loss and heat dissipation. AGMA technical paper, 1996.
[2] Weisbach J, Gordon L. Principles of the mechanics of machinery and engineering. In: Library of illustrated standard scientific works, vol. 2. H. Bailliere, Philadelphia, 1848.
[3] Reuleaux F. The constructor—a handbook of machine design. Henry Harrison Suplee. 1893.
[4] Buckingham E. Analytical mechanics of gears. Dover books for engineers. New York: McGraw-Hill Book Co.; 1949.
[5] Petry-Johnson TT, Kahraman A, Anderson NE, Chase DR. An experimental investigation of spur gear efficiency. J Mech Des 2008;130(6):062601. http://dx.doi.org/10.1115/1.2898876.
[6] Yenti C, Phongsupasamit S, Ratanasumawong C. Analytical and experimental investigation of parameters affecting sliding loss in a spur gear pair. Eng J 2013;17(1).
[7] DIN 3990: Tragfähigkeitsberechnung Von Stirnrädern: Anwendungsnorm für Industriegetriebe Detail-Methode, Beuth, 1989.
[8] Martins R, Seabra J, Brito A, Seyfert C, Luther A, Igartua R. Friction coefficient in fzg gears lubricated with industrial gear oils: biodegradable ester vs. mineral oil. Tribol Int 2006;39(6):512–21. http://dx.doi.org/10.1016/j.triboint.2005.03.021.
[9] Naruse C, Haizuka S, Nemoto R, Kurokawa K. Studies on frictional loss, temperature rise and limiting load for scoring of spur gear. Bull JSME 1986;29 (248):600–8. http://dx.doi.org/10.1299/jsme1958.29.600.
[10] Xiao L, Rosen B-G, Amini N, Nilsson PH. A study on the effect of surface topography on rough friction in roller contact. Wear 2003;254(11):1162–9. http://dx.doi.org/10.1016/S0043-1648(03)00329-6.
[11] Simrit: Radialwellendichtringe. Katalog no. 100.
[12] Fernandes C, Marques P, Martins R, Seabra J. Gearbox power loss. Part I: losses in rolling bearings. Tribol Int. 2015;88:298–308 http://dx.doi.org/10.1016/j.triboint.2014.11.017.

[13] Fernandes C, Marques P, Martins R, Seabra J. Gearbox power loss. Part II: friction losses in gears. Tribol Int. 2015;88:309–16 http://dx.doi.org/10.1016/j.triboint.2014.12.004.

[14] Fernandes C, Marques P, Martins R, Seabra J. Gearbox power loss. Part III: application to a parallel axis and a planetary gearbox. Tribol Int 2015;88:317–26 http://dx.doi.org/10.1016/j.triboint.2015.03.029.

[15] Durand De Gevigney J, Changenet C, Ville F, Velex P. Thermal modelling of a back-to-back gearbox test machine: application to the fzg test rig. Proc Inst Mech Eng Part J: J Eng Tribol 2012;226 (6):501–515. Cited by (since 1996) 3.

[16] Palmgren A. i. SKF industries. Ball and roller bearing engineering. SKF Industries, Philadelphia, 1959.

[17] SKF General Catalogue 6000 EN, SKF; November 2005.

[18] Cousseau T, Graça B, Campos A, Seabra J. Friction torque in grease lubricated thrust ball bearings. Tribol Int 2011;44(5):523–31. http://dx.doi.org/10.1016/j.triboint.2010.06.013.

[19] Gonçalves D, Pinho S, Graça B, Campos AV, Seabra J. Friction torque in thrust ball bearings lubricated with polymer greases of different thickener content. Tribol Int 2016;96:87–96 http://dx.doi.org/10.1016/j.triboint.2015.12.017.

[20] Fernandes CMCG, Marques PMT, Martins RC, Seabra JHO. Influence of gear loss factor on the power loss prediction. Mech Sci 2015;6(2):81–8. http://dx.doi.org/10.5194/ms-6-81-2015.

[21] Marques PM, Martins RC, Seabra JH. Power loss and load distribution models including frictional effects for spur and helical gears. Mech Mach Theory 2016;96(Part 1):1–25. http://dx.doi.org/10.1016/j.mechmachtheory.2015.09.005.

[22] Stribeck R. Die wesentlischen eigenschaften der gleit- und rollenlager. Pt I. Z Verein deutsch Ingen 1902;46(37):1341–8.

[23] Stribeck R. Die wesentlischen eigenschaften der gleit- und rollenlager. Pt II. Z Verein deutsch Ingen 1902;46(38):1432–8.

[24] Stribeck R. Die wesentlischen eigenschaften der gleit- und rollenlager. Pt III. Z Verein deutsch Ingen 1902;46(39):1463–70.

[25] Ohlendorf H. Verlustleistung und Erwärmung von Stirnrädern [Ph.D. thesis, dissertation]. TU München; 1958.

[26] Eiselt H. Beitrag zur experimentellen und rechnerischen bestimmung der fresstragfähigkeit von zahnradgetrieben unter berücksichtigung der zahnflankenreibung [Ph.D. thesis]. TH Desden; 1966.

[27] Matsumoto S, Asanabe S, Takano K, Yamamoto M. Evaluation method of power loss in high-speed gears. Jpn Soc Lubr Eng 1985:1165–70.

[28] Matsumoto S, Morikawa K. The new estimation formula of coefficient of friction in rolling–sliding contact surface under mixed lubrication condition for the power loss reduction of power transmission gears. In: International gear conference.

[29] Michaelis HWK. Scoring tests of aircraft transmission lubricants at high temperatures. J Synth Lubr 3(2) (1986).

[30] Schlenk L. Unterscuchungen zur Fresstragfähigkeit von Grozahnrädern [Ph.D. thesis, dissertation]. TU München; 1994.

[31] Höhn B-R, Michaelis K, Hinterstoißer M. Optimization of gearbox efficiency. goriva i maziva 2009;48(4):462–80.

[32] Misharin YA. Influence of the friction condition on the magnitude of the friction coefficient in the case of rollers with sliding. In: Proceedings international conference on gearing. Institute Mechanical Engineers.

[33] O'Donoghue JP, Cameron A. Friction and temperature in rolling sliding contacts. A S L E Trans 1966;9(2):186–94. http://dx.doi.org/10.1080/05698196608972134.

[34] Drozdov Y, Gavrikov Y. Friction and scoring under the conditions of simultaneous rolling and sliding of bodies. Wear 1968;11(4):291–302. http://dx.doi.org/10.1016/0043-1648(68)90177-4.

[35] Naruse C, Haizuka S, Nemoto R, Suganuma T. Studies on limiting load for scoring and frictional loss of hypoid gears of klingelnberg type. Bull JSME 1984;27(231):2053–60. http://dx.doi.org/10.1299/jsme1958.27.2053.

[36] Hai X. Development of a generalized mechanical efficiency prediction methodology for gear pairs [Ph.D. thesis]. The Ohio State University; 2005.

[37] Michaelis K. Die integraltemperatur zur beurteilung der fresstragfähigkeit von stirnrädern [Ph.D. thesis]. TU München; 1987.

[38] ISO/TR 14179-2:2001, Gears — Thermal capacity — Part 2: Thermal load-carrying capacity.

[39] Tallian TE. On competing failure modes in rolling contact. A S L E Trans 1967;10(4):418–39. http://dx.doi.org/10.1080/05698196708972201.

[40] Dowson D, Higginson G. Elasto-hydrodynamic lubrication: the fundamentals of roller and gear lubrication. The commonwealth and international library. Oxford: Pergamon Press; 1966.

[41] Brandão A, Meheux M, Ville F, Castro J, Seabra J. Experimental traction and stribeck curves of mineral, pao and ester based fully formulated gear oils. In: Proceedings of the 3rd international conference on integrity, reliability & failure, Porto, Portugal.

[42] Fernandes C, Marques P, Martins R, Seabra J. Film thickness and traction curves of wind turbine gear oils. Tribol Int. 2015;86:1–9 http://dx.doi.org/10.1016/j.triboint.2015.01.014.

[43] Benedict GH, Kelley BW. Instantaneous coefficients of gear tooth friction. A S L E Trans 1961;4(1):59–70. http://dx.doi.org/10.1080/05698196108972420.

[44] Diez-Ibarbia A, del Rincon A, Iglesias M, de Juan A, Garcia P, Viadero F. Efficiency analysis of spur gears with a shifting profile. Meccanica 2015:1–17. http://dx.doi.org/10.1007/s11012-015-0209-x.

[45] Rebbechi B, Oswald FB, Townsend DP. Dynamic measurements of gear tooth friction and load. In: Fall technical meeting of the American gear manufactures association; 1991.

[46] Fernandes C, Martins R, Seabra J, Blazquez L. FZG gearboxes lubricated with different formulations of polyalphaolefin wind turbine gear oils. In: Velex P, editor, International gear conference 2014: 26th–28th August 2014, Lyon. Oxford: Chandos Publishing; 2014. p. 699–708. http://dx.doi.org/http://dx.doi.org/10.1533/9781782421955.699.

[47] Fernandes C, Martins R, Seabra J. Torque loss of type C40 FZG gears lubricated with wind turbine gear oils. Tribol Int 2014;70:83–93.

[48] Fernandes C, Martins R, Seabra J. Friction torque of thrust ball bearings lubricated with wind turbine gear oils. Tribol Int 2013;58:47–54.

[49] Fernandes C, Martins R, Seabra J. Friction torque of cylindrical roller thrust bearings lubricated with wind turbine gear oils. Tribol Int 2013;59:121–8.

[50] Fernandes C, Amaro P, Martins R, Seabra J. Torque loss in thrust ball bearings lubricated with wind turbine gear oils at constant temperature. Tribol Int 2013;66:194–202.

[51] Fernandes C, Amaro P, Martins R, Seabra J. Torque loss in cylindrical roller thrust bearings lubricated with wind turbine gear oils at constant temperature. Tribol Int 2013;67:72–80.

[52] Marques P, Fernandes C, Martins R, Seabra J. Power losses at low speed in a gearbox lubricated with wind turbine gear oils with special focus on churning losses. Tribol Int 2013;62:186–97.

[53] Marques PM, Fernandes CM, Martins RC, Seabra JH. Efficiency of a gearbox lubricated with wind turbine gear oils. Tribol Int 2014;71:7–16.

[54] Michaelis K, Höhn B-R. Influence of lubricants on power loss of cylindrical gears. Tribol Trans 1994;37(1):161–7. http://dx.doi.org/10.1080/10402009408983279 arXiv:.

[55] Kyotani T, Yoshitake H, Ito T, Tamai Y. Correlation between flow properties and traction of lubricating oils. A S L E Trans 1986;29(1):102–6. http://dx.doi.org/10.1080/05698198608981665.

[56] Igarashi J, Kagaya M, Satoh T, Nagashima T. High viscosity index petroleum base stocks—the high potential base stocks for fuel economy automotive lubricants. Technical report; February 1992. http://dx.doi.org/10.4271/920659.

[57] Sasaki T, Ohmori I, Furumoto M, Tanaka H, Komiya K, Ohsumi T, et al. Development of automotive lubricants based on high-viscosity index base stock. Technical report; February 1995. http://dx.doi.org/10.4271/951028.

[58] AGunsel S, Korcek S, Smeeth M, Spikes HA. The elastohydrodynamic friction and film forming properties of lubricant base oils. Tribol Trans 1999; 42(3):559–69. http://dx.doi.org/10.1080/10402009908982255.

[59] Brandão AJ, Meheux M, Ville F, Castro MJD, Seabra J. Traction curves and rheological parameters of fully formulated gear oils. Proc Inst Mech Eng Part J: J Eng Tribol 2011;225(7):577–93 http://dx.doi.org/10.1177/1350650111405111.

[60] Fernandes CM, Battez AH, González R, Monge R, Viesca J, García A, et al. Torque loss and wear of FZG gears lubricated with wind turbine gear oils using an ionic liquid as additive. Tribol Int 2015;90(0):306–14. http://dx.doi.org/10.1016/j.triboint.2015.04.037.

[61] ASTM D341-09. Standard practice for viscosity–temperature charts for liquid petroleum products.

[62] Gold PW, Schmidt A, Dicke. H, Loos J, Assmann C. Viscosity–pressure–temperature behavior of mineral and synthetic oils. J Synth Lubr 2001;18(1):51–79.

[63] Mia S, Mizukami S, Fukuda R, Morita S, Ohno N. High-pressure behavior and tribological properties of wind turbine gear oil. J Mech Sci Technol 2010;24 (1):111–4.